

IDENTIFYING THE CONDITIONS FOR MINIMUM PITTING CORROSION IN FRICTION STIR WELDED DISSIMILAR JOINTS OF ALUMINIUM – MAGNESIUM ALLOYS

^{*1}R.KAMAL JAYARAJ, ²S. MALARVIZHI, ³V.BALASUBRAMANIAN

^{*1}R.Kamal Jayaraj

Research Scholar, Centre for Materials Joining and Research (CEMAJOR), Department of Manufacturing Engineering, Annamalai University, Annamalai Nagar – 608 002, Tamil Nadu, India.

jayaraj_kamal@yahoo.co.in

²Dr. S. Malarvizhi

Associate Professor, Centre for Materials Joining and Research (CEMAJOR), Department of Manufacturing Engineering, Annamalai University, Annamalai Nagar – 608 002, Tamil Nadu, India.

jeejoo@rediffmail.com

³Dr. V.BALASUBRAMANIAN (Corresponding Author)

Professor,

Centre for Materials Joining and Research (CEMAJOR), Department of Manufacturing Engineering, Annamalai University, Annamalai Nagar – 608 002, Tamil Nadu, India.

visvabalu@yahoo.com

Abstract

In automobile industries aluminium (Al) and magnesium (Mg) alloys are to be joined to reduce the weight of vehicle and to increase the fuel efficiency. Friction stir welding (FSW), is a solid state joining process, has capable of joining Al/Mg alloys. The influences of material flow and formation of intermetallics in the weld nugget are responsible for deteriorating the corrosion behaviour of weld nugget. The potential difference between aluminium and magnesium in their galvanic couple can accelerate the initiation of pitting corrosion on magnesium alloy. In this investigation, the conditions for minimizing pitting corrosion in friction stir welded dissimilar joints of aluminium and magnesium alloys were identified by response surface methodology (RSM). Incorporating chloride ion concentration, pH and exposure time a quadratic model was developed to predict pitting corrosion rate. The minimum corrosion attack was observed under following conditions of 0.36 M chloride ion concentration, pH of 4.62 and 15 mins of exposure time.

Key words: Friction stir welding, Dissimilar joint, Aluminium alloy, Magnesium alloy, Pitting corrosion, Response surface methodology.

Introduction

Aluminium (Al) alloys are a light weight metal which is widely used in automobile industries and structural applications [1]. Now a days, weight reduction is the main task in automotive industries to reduce air pollution and fuel consumption. Therefore, attraction of industries moves towards on magnesium (Mg) alloys because of their lower density and high specific strength [2]. Welding of Al/Mg dissimilar joints by fusion welding processes is very difficult due to differences in melting point, crystal structure and chemical composition [3]. Therefore, friction stir welding (FSW) is used to join Al/Mg dissimilar joints; in this process low heat input is sufficient to weld the metals [4]. In weld zone the materials are mixed together and formed an intercalated microstructure [5]. Potential differences between these two metals in their galvanic couple can accelerate the pitting corrosion to least potential metal [6].

The corrosion behaviour of friction stir welds of Al alloys was investigated by few researchers. Bala Srinivasan et al. [7] found that the parent alloy AA 2219 and the friction stir welded joint both exhibited good resistance to stress corrosion cracking in 3.5% NaCl solution. The corrosion behaviour of friction stir welded AA 2050 alloy joint was studied using conventional immersion test and stationary electrochemical technique [8]. The results obtained in this work showed that the weld nugget was susceptible to both intergranular and intragranular corrosion. It is well known that Mg alloys are susceptible to localized corrosion such as pitting and stress corrosion cracking (SCC) [9–11]. Few investigations were carried out on friction stir welded of magnesium alloys. An empirical relationship was developed to predict the corrosion rate of friction stir welded AZ61A Mg alloy [12]. From the results, it is understood that the increase in immersion time resulting in hydroxide layer formed on the surfaces and reduces the further corrosion attack.

In recent times, significant amount of work has been undertaken on the mechanical properties and microstructural evolution of dissimilar friction stir welds of Al/Mg alloys [13, 14]. Joining of dissimilar alloys by FSW results in intercalated microstructure in stir zone [15]. The occurrence of galvanic corrosion was due to the formation of Mg/Al galvanic couples with a small ratio of anode-to-cathode surface area. The corrosion product was primarily the porous magnesium hydroxide with characteristic microcracks and exhibited a low microhardness value. Compared with similar FSW joints, dissimilar FSW joints corrode severely. So, it is important to indentify the conditions that will lead to minimum corrosion rate in weld nugget region of friction stir welded Al/Mg dissimilar joints. There is no literature available till date to identify the conditions for minimum corrosion rate in dissimilar joints made by FSW process. Hence, in this investigation, an attempt has been

made to identify the conditions for minimizing pitting corrosion rate in friction stir welded dissimilar joints of AA6061 Al and AZ31B Mg alloys under NaCl environment by response surface methodology (RSM).

Experimental Work

Fabrication of joints and specimen preparations

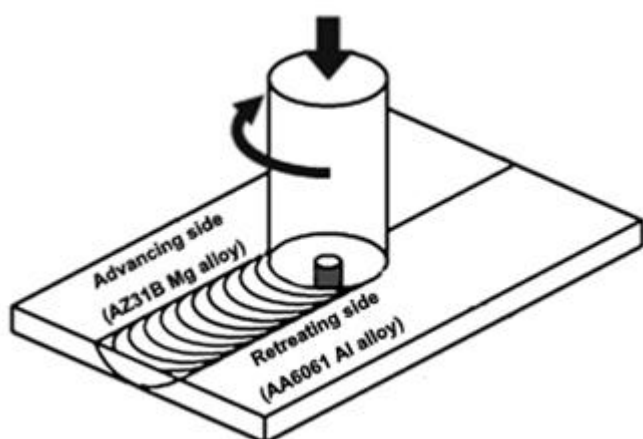
A 6 mm thick rolled plates of AZ31B Mg alloy and AA6061-T6 Al alloy plates were used as base materials in this investigation. The chemical compositions of these alloys are listed in Table 1. To fabricate FSW joint, the plates were cut to the required size (150 mm x 75 mm) by power hacksaw. A square butt joint was obtained by securing the plates in position using mechanical clamps. The welding direction was normal to the rolling direction of the plates. Fig. 1a shows the positioning of the plates during welding; AA6061 aluminium alloy is placed in the retreating side and AZ31B magnesium alloy in advancing side. Taper threaded cylindrical tool made of super high speed steel (Fig. 1b) was used to fabricate the joints.

Table 1 Chemical composition (wt. %) of AA6061 aluminium and AZ31B magnesium alloys

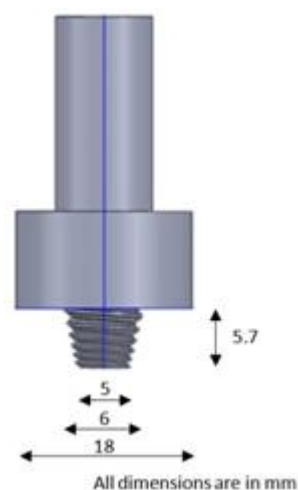
Alloy	Al	Zn	Si	Mn	Cu	Cr	Mg
AA6061	Bal	–	0.6	–	0.25	0.2	1.0
AZ31B	3.0	1.0	0.1	0.6	0.04	–	Bal

A computer numerical controlled (CNC) friction stir welding machine (22 kW; 4000 rpm; 60 kN) was used to fabricate the joints. From literature [16], the optimized welding parameters and tool dimensions were taken.

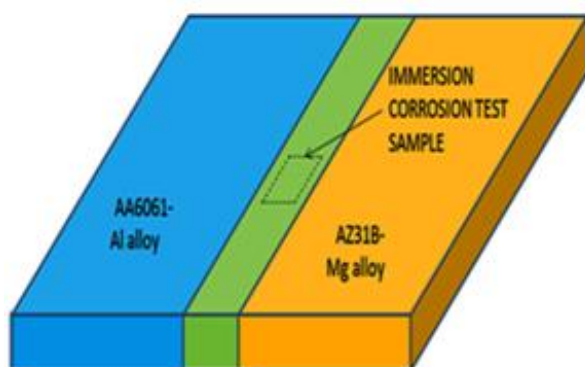
From the fabricated joints, the specimens were extracted from weld nugget region of the FSW joints for conducting potentiodynamic polarisation test with the dimensions of 20 x 20 x 6 mm. The scheme of extraction of corrosion test samples is shown in Fig. 1c. Before corrosion test, the specimens were grounded and polished with 600 to 1500 grit SiC paper. Finally, it was cleaned with acetone and washed in distilled water and then dried by warm flowing air. The photograph of the polished corrosion test specimen is shown in Fig. 1d. The sample placed in a pitting corrosion test cell is shown in Fig. 1e. The Gill-AC potentiostat instrument was used to conduct the potentiodynamic polarization test in NaCl solution at different conditions as shown in Fig. 1f. The optical micrograph of parent metals and stir zone of dissimilar friction stir welded joint are shown in Fig. 2.



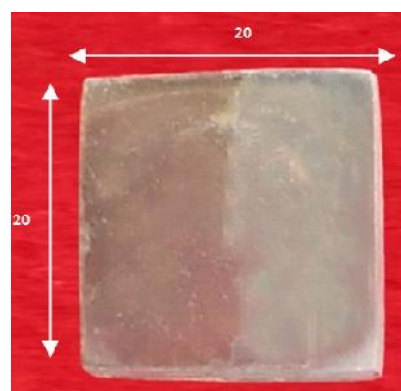
a. FSW of dissimilar joint (Schematic diagram)



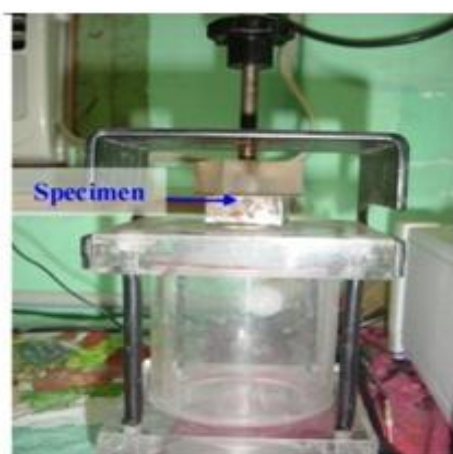
b. Tool dimensions



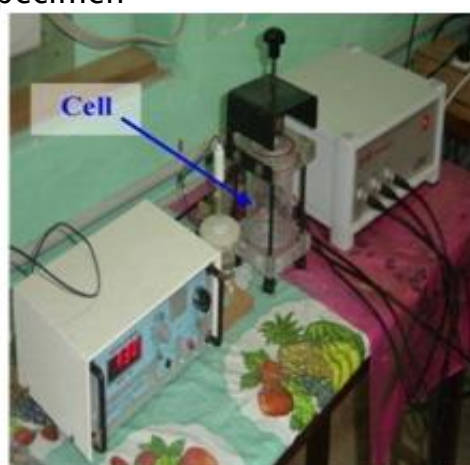
c. Specimen extraction scheme



d. Dimension of pitting corrosion test specimen



e. Pitting corrosion test cell



f. Gill AC Potentiostat

Fig.1 Experimental details

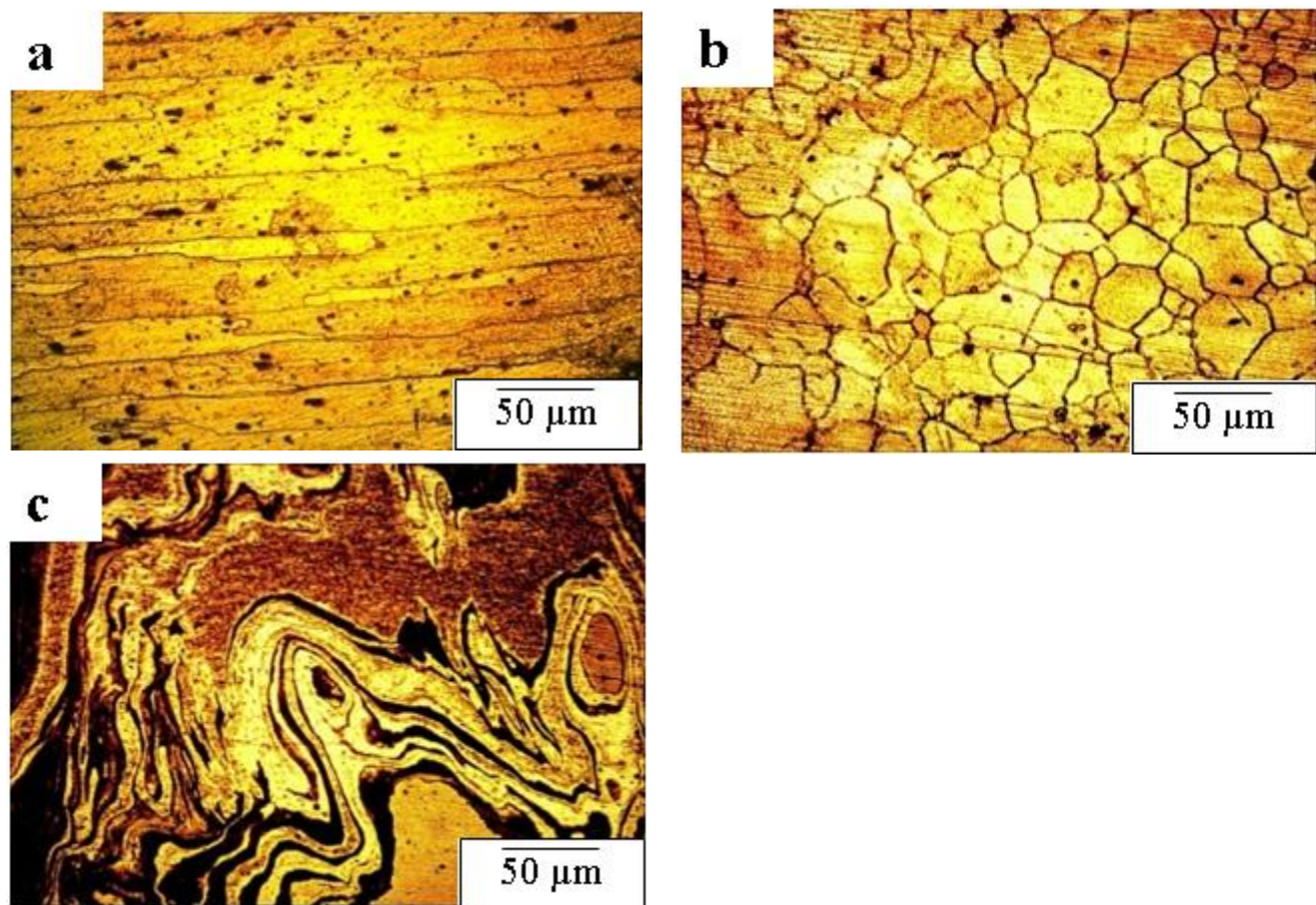


Fig 2. Optical micrograph of (a) AA6061 aluminium (b) AZ31B magnesium alloy and (c) weld nugget region of friction stir welded dissimilar joints.

Selection of experimental design matrix

A central composite rotatable three-factor, five level factorial design matrix was selected to minimize number of experiments. The experimental design matrix consisting 20 sets of coded conditions, comprising a full replication three-factor factorial design of eight points, six star points, and six center points was used. Table 2 presents the range of factors considered and Table 3 shows the 20 sets of actual values and output responses of the experiments. The lower and upper limits of the parameters were coded as -1.682 and $+1.682$, respectively. Thus, the 20 experimental runs allowed for the estimation of the linear, quadratic, and two-way interactive effects of the variables. The way of designing such a matrix is dealt with elsewhere [17, 18].

The coded values for intermediate levels can be calculated from the relationship.

$$X_i = \frac{1.682[2X - (X_{\max} + X_{\min})]}{X_{\max} - X_{\min}} \quad (1)$$

Where X_i is the required coded value of a variable X and X is any value of the variable from X_{\min} to X_{\max} ; X_{\min} is the lower level of the variable; X_{\max} is the upper level of the variable.

Table 2. Important factors and their levels

S.No.	Factor	Notation	Unit	Levels				
				-1.68	-1	0	+1	+1.68
1	Chloride ion con.	C	Mol	0.2	0.36	0.6	0.84	1
2	pH value	P	–	3	4.62	7	9.38	11
3	Exposure time	T	mins	5	15	30	45	55

Pitting corrosion rate evaluation

NaCl solutions with concentrations of 0.2, 0.36, 0.6, 0.84 and 1 mol/L were prepared. The pH value was measured using a digital pH meter and varied from 3 to 11 as prescribed by design matrix. The corrosion rate of the weld nugget region was calculated from current density multiplied by a metal factor. The expression is followed as,

$$\text{Corrosion rate, mm/year} = \frac{\text{Metal factor} \times i_{\text{corr}}}{1000} \quad (2)$$

The current density (i_{corr}) is expressed as,

$$i_{\text{corr}} (\text{A/m}^2) = \frac{b_a \times b_c}{2.3 \times R_p \times (b_a + b_c)} \quad (3)$$

Where, b_a is anodic tafel slope in volts, b_c is the cathodic tafel slope in volts and R_p is the polarization resistance in Ω/m^2 .

Metal factor is calculated from,

$$\text{Metal factor} = \frac{t \times K}{\rho} \quad (4)$$

Where 't' is the seconds in year, 'ρ' is the density in g/cm^3 and 'K' is the electrochemical equivalent in g/coulombs . From equation (2) the pitting corrosion rates were calculated and the results were tabulated in Table. 3.

Table 3. Design matrix and experimental results

Exp. No.	Actual values			Output responses		
	Con. (C)	pH (P)	Time (T)	I_{corr} (mA/cm ²)	E_{corr} (mVSCE)	CR (mm/year)
1	0.36	4.62	15	0.96	-1359	15.11
2	0.84	4.62	15	2.26	-1542	34.99
3	0.36	9.38	15	1.03	-1559	16.16
4	0.84	9.38	15	2.16	-1484	34.12
5	0.36	4.62	45	2.02	-1445	23.02
6	0.84	4.62	45	2.03	-1524	23.65
7	0.36	9.38	45	1.90	-1516	19.99
8	0.84	9.38	45	1.49	-1414	18.33
9	0.20	7.00	30	0.95	-1371	14.98
10	1.00	7.00	30	2.12	-862	33.32
11	0.60	3.00	30	1.92	-1540	22.07
12	0.60	11.00	30	1.46	-1138	18.17
13	0.60	7.00	5	2.12	-816	30.52
14	0.60	7.00	55	2.10	-1391	25.05
15	0.60	7.00	30	1.68	-1313	18.68
16	0.60	7.00	30	1.16	-1027	16.20
17	0.60	7.00	30	1.19	-1451	16.54
18	0.60	7.00	30	1.50	-988	18.54
19	0.60	7.00	30	1.40	-1163	17.62
20	0.60	7.00	30	1.27	-1054	17.08

Developing an Empirical Relationship

A second order quadratic model was developed to correlate the pitting corrosion test parameters. The response (corrosion rate) is a function of chloride ion concentration (C), pH value (P), and exposure time (T).

$$\text{Pitting corrosion rate} = f\{C, P, T\} \quad (5)$$

The equation should contain main and interaction effects of all variables and hence the response is expressed as

$$Y = b_0 + \sum b_i x_i + \sum b_{ii} x_i^2 + \sum b_{ij} x_i x_j \quad (6)$$

For three factors, the selected response could be expressed as

$$PCR = b_0 + b_1(C) + b_2(P) + b_3(T) + b_{12}(CP) + b_{13}(CT) + b_{23}(PT) + b_{11}(C^2) + b_{22}(P^2) + b_{33}(T^2) \quad (7)$$

Where, b_0 is the average of responses (corrosion rate) and $b_1, b_2, b_3, \dots, b_{11}, b_{12}, b_{13}, \dots, b_{22}, b_{23}, b_{33}$ are the coefficients that depend on their respective main and interaction factors, which were calculated using the expression given below,

$$B_i = \sum (X_i, Y_i) / n \quad (8)$$

where 'i' varies from 1 to n, in which X_i is the corresponding coded value of a factor and Y_i is the corresponding response output value (corrosion rate) attained from the experiment and 'n' is the total number of combination considered. All the coefficients were calculated by applying central composite face centred design using the Design Expert statistical software package. The significance of each co-efficient was calculated by student's t-test and p-values, which are presented in Table 4; Values of "Prob >F" less than 0.05 indicate that the model terms are significant.

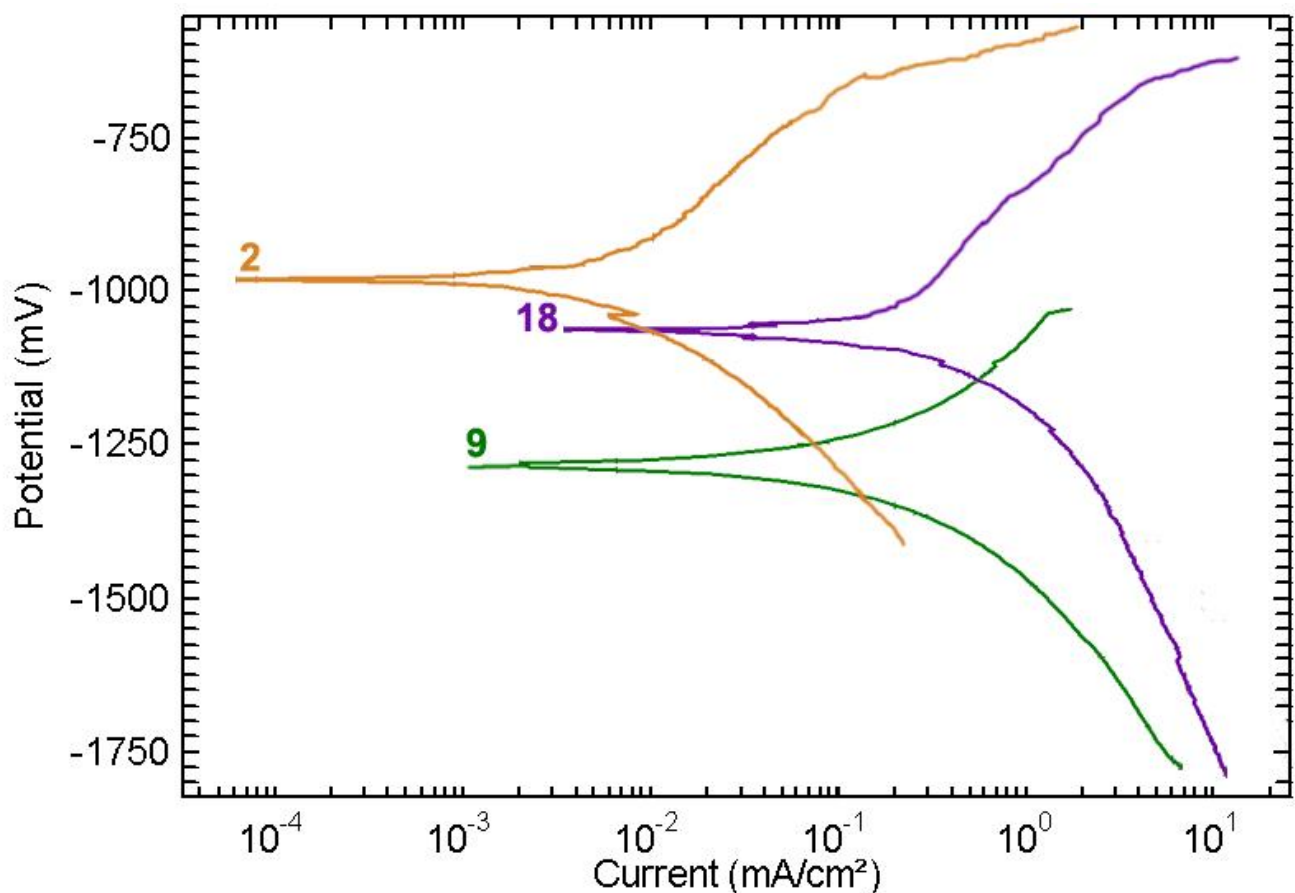


Fig. 3 Potentiodynamic polarization curves for Al/Mg FSW dissimilar joints of WZ tested in different conditions of NaCl solution.

After determining the significant coefficients (at 95 % confidence level), the final relationship was developed by using these coefficients. The final empirical relationship derived by the above method to estimate the pitting corrosion rate of nugget region (stir zone) of friction stir welded Al/Mg dissimilar joint is given below,

$$\text{Pitting corrosion rate } \left(\frac{\text{mm}}{\text{year}} \right) = 9.96 + 23.85(C) - 0.68(P) - 6.64(T) - 0.93(CP) - 1.37(CT) - 0.03(PT) + 37.26(C^2) + 0.12(P^2) + 0.02(T^2) \quad (9)$$

Table 4. Calculated values of coefficients

Coefficient	Factor Estimate
Intercept	9.96
C	23.85
P	0.68
T	6.64
CP	0.93
CT	1.37
PT	0.03
C ²	37.26
P ²	0.12
T ²	0.02

The analysis of variance (ANOVA) technique was used to find the significant main and interaction factors. The ANOVA results for second order response surface model fitting are given in the Table 5. The determination coefficient (r^2) indicated the goodness of fit for the model. The model F-value of 68.90 implies the model is significant. There is only a 0.01% chance that a "Model F-Value" this large could occur due to noise. Values of "Prob > F" less than 0.0500 indicate model terms are significant. In this case C, P, T, CT, PT, C², P², T² are significant model terms.

Values greater than 0.1000 indicate the model terms are not significant. If there are many insignificant model terms (not counting those required to support hierarchy), model reduction may improve the model. The "Lack of Fit F-value" of 1.48 implies the lack of fit is not significant relative to the pure error. There is a 33.96% chance that a "Lack of Fit F-value" this large could occur due to noise. Non-significant lack of fit is good. The "Pred R-Squared" of 0.9192 is in reasonable agreement with the "Adj R-Squared" of 0.9698. "Adeq Precision" measures the signal to noise ratio, a ratio greater than 4 is desirable. Ratio of 25.656 indicates an adequate signal. Each observed value is compared with the predicted value calculated from the model is shown in the Fig. 4.

Table 5. ANOVA test results

Source	Sum of squares	Df	Mean square	F value	p-value Prob>F	
Model	807.75	9	89.75	68.90	< 0.0001	Significant
<i>C</i>	335.26	1	335.26	257.37	< 0.0001	
<i>P</i>	15.91	1	15.91	12.21	0.0058	
<i>T</i>	44.27	1	44.27	33.99	0.0002	
<i>CP</i>	2.211	1	2.21	1.70	0.2218	
<i>CT</i>	188.84	1	188.84	144.97	< 0.0001	
<i>PT</i>	9.12	1	9.12	7.00	0.0245	
<i>C²</i>	64.04	1	64.04	49.16	< 0.0001	
<i>P²</i>	6.72	1	6.72	5.16	0.0465	
<i>T²</i>	165.98	1	165.98	127.42	< 0.0001	
Residual	13.03	10	1.30			
Lack of Fit	7.77	5	1.55	1.48	0.3396	<i>not significant</i>
<i>Pure Error</i>	5.26	5	1.05			
Cor Total	820.78	19				

Identifying Minimum Pitting Corrosion Conditions

Figure 6a is a 3D response graph and contour graph shows the interaction effect of chloride ion concentration and pH. When pH is compared with chloride ion concentration, PH has insignificant effect on corrosion rate as illustrated in Fig. 6a. When the chloride ion concentration increases there is significant increase in corrosion rate. Especially, the corrosion rate dependent on current density when the icorr increases the corrosion rate also increases. Interaction effect of chloride ion concentration and exposure time is shown in Figure 6b. The interaction effect between these two factor is more significant than the interaction effect between the other combinations of parameters. In pitting corrosion, the chloride ion concentration is more sensitive factor than other parameters. Figure 6c illustrates interaction effect of pH and exposure time on Al/Mg dissimilar FSW joint. As can be seen, pH has insignificant effect on corrosion rate when the exposure time is low. But, simultaneously increase in time with lower pH gives rise to a considerable increase in corrosion rate.

From the surface and contour plots the minimum corrosion rate conditions were identified as shown is Fig. 6. The least point in response plot shows the minimum achievable corrosion rate. A contour plot is formed to display the minimum corrosion rate parameter setting visually for second order responses, such a plot can be more complex compared to

the simple series of parallel lines that can occur with first order models. Once the stationary point is found, it is usually necessary to characterize the response surface in the immediate vicinity of the point. Identification involves whether the stationary point is a minimum response or maximum response or a saddle point to classify this; it is straight forward to analyze it through a contour plot. Contour plot plays a very important role in the study of a response surface. It is clear from that when the corrosion rate increases with increase in pH value up to certain level and then decreases.

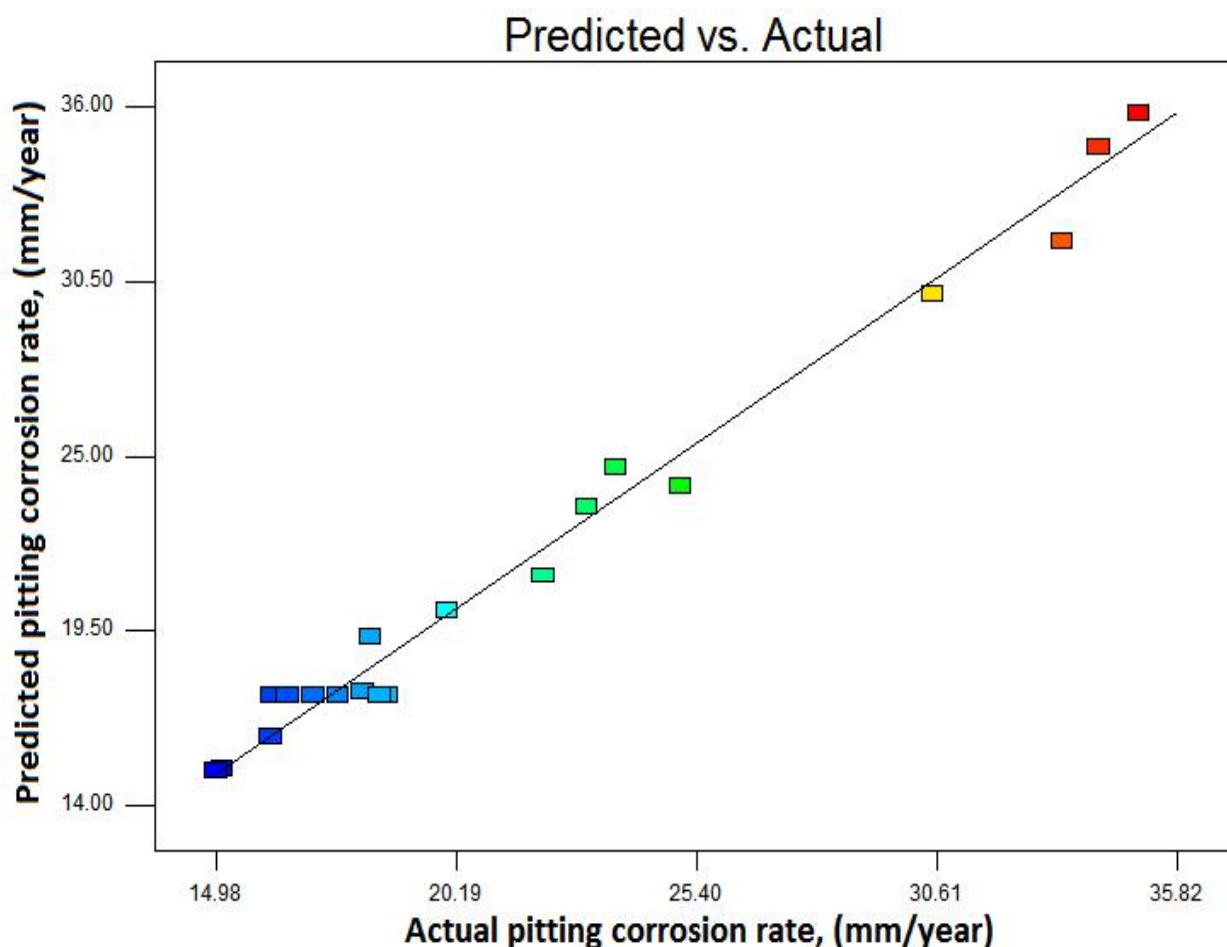
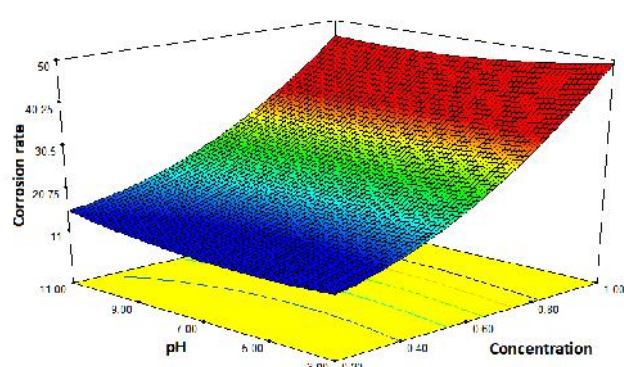
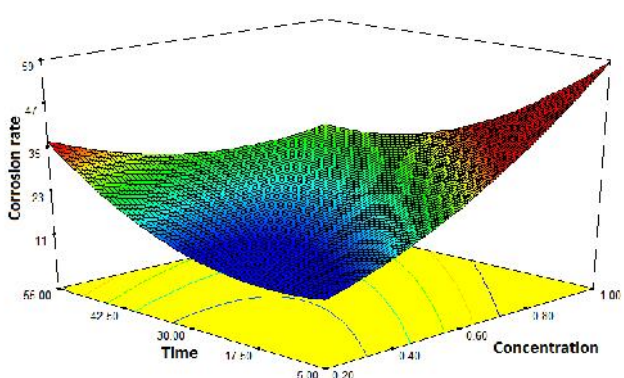
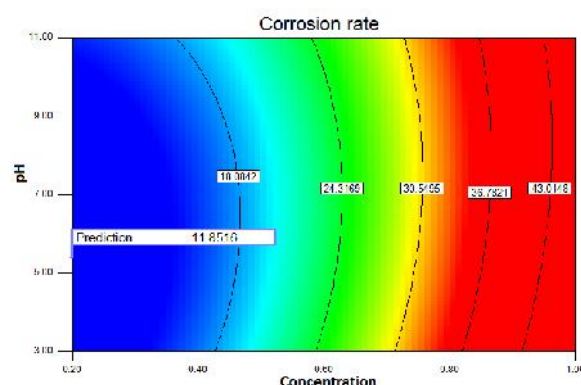


Fig. 4 Correlation graph

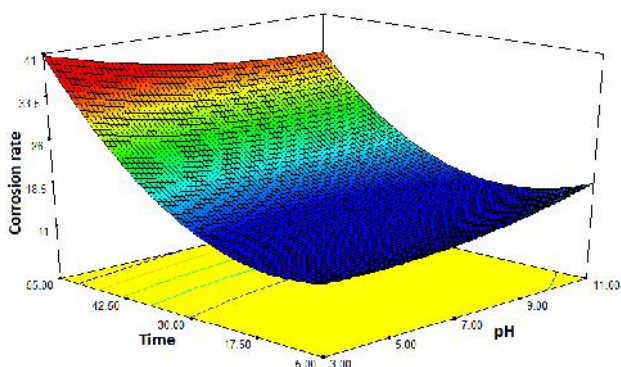
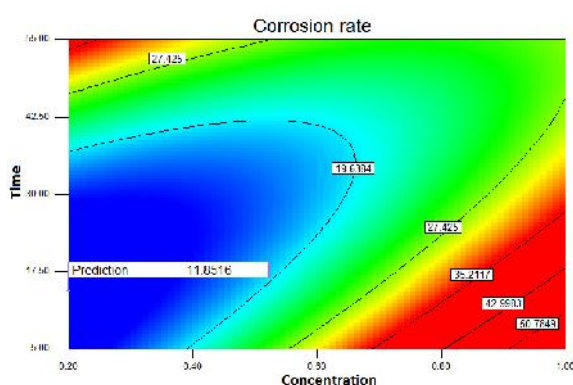
By analyzing the response surface and contour plots as shown in Fig.6 (a–c), the minimum achievable corrosion rate value is found to be 11.85 mm/year. The corresponding parameters that give up this minimum value are chloride ion concentration of 0.20 (Mol), pH value of 5.39 and exposure time of 14.48 mins. The lower F ratio value implies that the respective levels are less significant. From the F ratio value, it can be concluded that the chloride ion concentration is contributing the major factor to corrosion attack, followed by exposure time and pH value for the range considered in this investigation.



(a) Interaction effect of chloride ion concentration and pH.



(b) Interaction effect of chloride ion concentration and exposure time.



(c) Interaction effect of pH and exposure time.

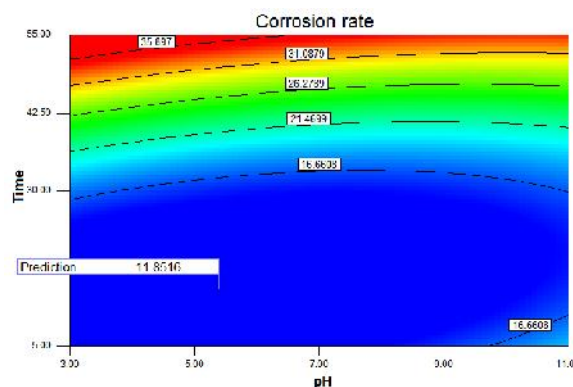


Fig. 5 Response surface graphs and contour plots

To validate the developed relationship, three confirmation experiments were conducted by varying the concentration of chloride ion, pH and exposure time; the values were chosen randomly within the range of test parameters presented in Table 2. The actual response was calculated from the average of three measured results. Table 6 summarizes the experimental values, predicted values and the variation. The validation results revealed that the developed empirical relationship is quite accurate as the variation is $\pm 2\%$.

Table 6. Validation test results

Si.No	Chloride ion concentration, (Mol)	pH	Exposure time, (mins)	Actual corrosion rate (mm/year)	Predicted corrosion rate (mm/year)	Variation (%)
1	0.4	5	6	19.72	19.67	0.05
2	0.5	4	11	21.86	22.00	-0.14
3	0.9	9	7	48.33	48.06	0.27

The potentiodynamic polarization test was performed to evaluate the corrosion behavior of weld nugget of FSWed dissimilar joints of aluminium – magnesium alloys in different solutions. From the 20 experiments, only 3 curves (low, medium and high corrosion rates) were illustrated in Fig. 3. From this polarization curve current density (i_{corr}) and corrosion potential (E_{corr}) were noted as listed in table 3. The corrosion rate dependent on corrosion current density when the i_{corr} increases the corrosion rate also increases.

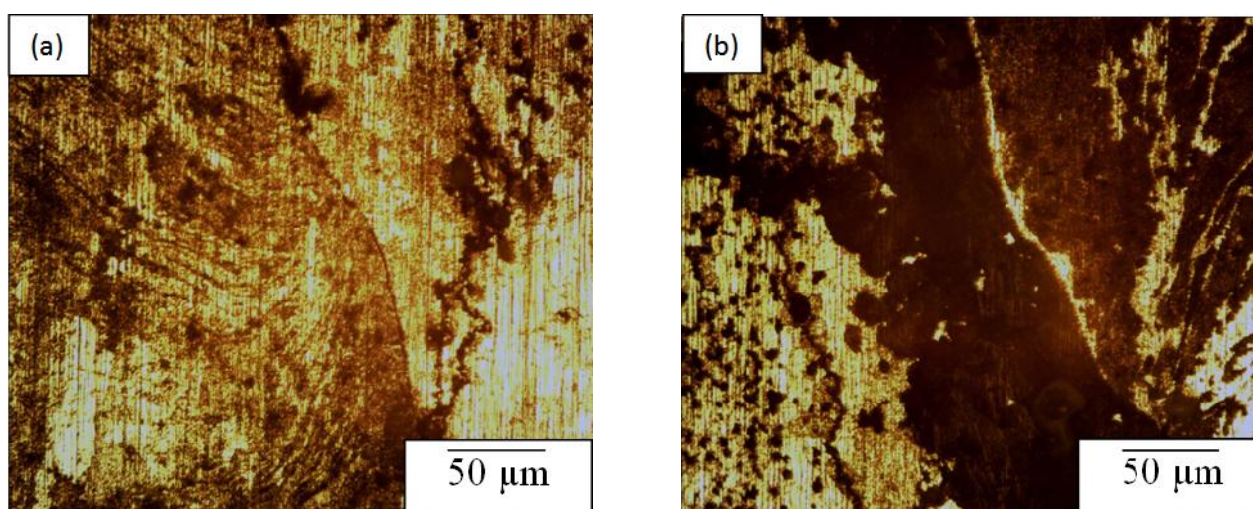


Fig. 6 Optical micrograph of the corrosion test specimens (a) Minimum corrosion attack (b) Maximum corrosion attack.

Fig. 6 shows the optical micrograph of the corrosion test specimens exhibited minimum and maximum corrosion rates. In both the conditions, magnesium alloy corrode severely than aluminium alloy, this may be due to differences in potential between these two alloys. In this magnesium alloy has more negative potential than aluminium alloy, so magnesium alloy is more active than aluminum alloy. From all the experimental conditions, minimum corrosion attack observed in a chloride ion concentration of 0.36 Mol, pH of 4.62 and

exposure time of 15 mins. It is clearly visible in Fig. 6(a), few surfaces on magnesium side corroded by potentiodynamic test and no visible attack observed in aluminium side. Hence, maximum corrosion attack observed in a chloride ion concentration of 0.84 Mol, pH of 4.62 and exposure time of 15 mins. It is seen in Fig. 6(b), the large surfaces of the magnesium alloy corroded when it is involved to potentiodynamic test.

Conclusions

- (i) An empirical relationship was developed to predict the corrosion rate of weld nugget region of friction stir welded dissimilar joints of AA6061 Al – AZ31B Mg alloys with 95% of confidence level. The relationship was developed incorporating the chloride ion concentration, pH value of environment and exposure time using statistical tools, such as design of experiments and regression analysis.
- (ii) Response surface method was used to optimize the pitting corrosion parameters to attain minimum corrosion rate in the weld nugget region of friction stir welded dissimilar joints of AA6061 Al – AZ31B Mg alloys.
- (iii) The results indicate that the chloride ion concentration has a significant effect on the corrosion rate. By optimization the minimum corrosion rate 11.85 mm/year was identified, it obtained in the conditions of 0.20 M chloride ion concentration, 5.39 of pH and 14.48 mins of exposure time.

Acknowledgements

The authors wish to express sincere thanks to Council of Scientific and Industrial Research (CSIR), New Delhi for the financial support to carry out this investigation through sponsored project No. 22(0615)/13/EMR-II dated 26.02.2013.

References

- [1] 'Physical Metallurgy and Processes', E. George Totten and D. Scott MacKenzie, *Handbook of Aluminum*, Marcel Dekker, Inc., New York, 7, 2003.
- [2] 'Welding and joining of magnesium alloys', Liming Liu, *Woodhead Publishing Limited*, UK, 2010.
- [3] 'Friction Stir Welding of Dissimilar Alloys and Materials', Nilesh Kumar, Wei Yuan and S. Rajiv Mishra, *Butterworth-Heinemann publications*, Elsevier Inc., USA, 2015.
- [4] 'Friction stir welding process of dissimilar metals of 6061-T6 aluminum alloy to AZ31B magnesium alloy', Banglong Fu, Guoliang Qin, Fei Li, Xiangmeng Meng, Jianzhong Zhang and Chuansong Wu, *Journal of Materials Processing Technology*, 218, pp38-47, 2015.

- [5] 'Microstructures in friction–stir welded dissimilar magnesium alloys and magnesium alloys to 6061–T6 aluminum alloy', A.C. Somasekharan and L.E. Murr, *Materials Characterization*, **52**, pp49–64, 2004.
- [6] 'Polishing–assisted galvanic corrosion in the dissimilar friction stir welded joint of AZ31 magnesium alloy to 2024 aluminum alloy', C. Liu, D.L. Chen, S. Bhole, X. Cao and M. Jahazi, *Materials Characterization*, **60**, pp370– 376, 2009.
- [7] 'Characterisation of microstructure, mechanical properties and corrosion behaviour of an AA2219 friction stir weldment', P. Bala Srinivasan, K.S. Arora, W. Dietzel, S. Pandey and M.K. Schaper, *Journal of Alloys and Compounds*, **492**, pp631–637, 2010.
- [8] 'Characterisation and understanding of the corrosion behaviour of the nugget in a 2050 aluminium alloy Friction Stir Welding joint', Vincent Proton, Joel Alexis, Eric Andrieu, Jerome Delfosse, Marie–Christine Lafont and Christine Blanc, *Corrosion Science*, **73**, pp130–142, 2013.
- [9] 'Testing of general and localized corrosion of magnesium alloys: A critical review' E. Ghali, W. Dietzel and K.U. Kainer, *Journal of Materials Engineering and Performance*, **13**,5, pp517–529, 2004.
- [10] 'A critical review of the stress corrosion cracking(SCC) of magnesium alloys', N. Winzer, A. Atrens, G. Song, E. Ghali, W. Dietzel, K.U. Kainer, N. Hort and C. Blawert, *Advanced Engineering Materials*. **7**, pp659, 2005.
- [11] 'A study on stress corrosion cracking and hydrogen embrittlement of AZ31 magnesium alloy', R.G. Song, C. Blawert, W. Dietzel, A. Atrens, *Materials Science and Engineering A*, **399**, pp308, 2005.
- [12] 'Corrosion behaviour of friction stir welded AZ61A magnesium alloy welds immersed in NaCl solutions', A. Dhanapal, S. Rajendra Boopathy and V. Balasubramanian, *Transactions of Nonferrous Metals Society of China*, **22**, pp793–802, 2012.
- [13] 'Dissimilar friction stir welding between 5052 aluminum alloy and AZ31 magnesium alloy', Yan Yong, Zhang Da–tong, Qiu Cheng and Zhang Wen, *Transactions of Nonferrous Metals Society of China*, **20**, pps619–s623, 2010.
- [14] 'Microstructure of friction stir welding of aluminium alloy to magnesium alloy', A. Kostka, R.S. Coelho, J. Dos Santos and A.R. Pyzalla, *Scripta Materialia*, **60**, pp953–956, 2009.

- [15] 'Microstructure characteristics and performance of dissimilar welds between magnesium alloy and aluminum formed by friction stirring', Jiuchun Yan, Zhiwu Xu, Zhiyuan Li, Lei Li and Shiqin Yang, *Scripta Materialia*, **53**, pp585–589, 2005.
- [16] 'Influences of tool shoulder diameter to plate thickness ratio (D/T) on stir zone formation and tensile properties of friction stir welded dissimilar joints of AA6061 aluminum–AZ31B magnesium alloys', S. Malarvizhi and V. Balasubramanian, *Materials and Design*, **40**, pp453–460, 2012.
- [17] 'Response surfaces', A.I. Khuri and J.A. Cornell, 2nd edition, Marcel Dekker, New York, 1996.
- [18] 'Probability and Statistics for Engineers', R.G. Miller, J.E. Freund and D.E. Johnson, *Prentice of Hall of India Private Limited*, New Delhi, 1999.